

Supporting Information

Visible-light-driven photo-Fenton degradation of ceftriaxone sodium using SnS₂/LaFeO₃ composite photocatalysts

New Journal of Chemistry

Yuting Guo^a, Cong Chen^a, Liwei Ling^a, Jun Wang^a, Huixiu Qi^a,

Bingjie Zhang^a, Min Wu^{*a}

^a School of Chemistry and Chemical Engineering, Southeast University, Nanjing 211189, P. R. China

* Corresponding Author: Min Wu E-mail: wuminnj@163.com

Experimental

Chemicals and materials

Iron nitrate nonahydrate (Fe (NO₃)₃·9H₂O, AR), Lanthanum nitrate hexahydrate (La (NO₃)₃·6H₂O, AR) and Tin (IV) chloride pentahydrate (SnCl₄·5H₂O, AR) were purchased from Aladdin Co., Ltd. Citric acid monohydrate (C₆H₈O₇·H₂O, AR), Thiourea (AR), Ethylene glycol (EG, AR) were provided by Sinopharm Chemical Reagent Co., Ltd. Ceftriaxone sodium (AR) were obtained from Shanghai Macklin Biochemical Co., Ltd. All reagents were received without any further treatment, and deionized water was used for all the study.

Preparation of pure LaFeO₃, SnS₂ photocatalysts

Pure LaFeO₃ particles were prepared through the citric acid sol-gel method according to the modified literature procedure.¹ Initially, Fe (NO₃)₃·9H₂O (2.0200 g, 5

mmol) and $\text{La}(\text{NO}_3)_3 \cdot 6\text{H}_2\text{O}$ (2.1650 g, 5 mmol) were dissolved in 50 mL of deionized water to form an orange solution. After dissolved in 30 mL of deionized water, citric acid (2.1014 g, 10 mmol) was slowly dropped into the above mixture under magnetic stirring. Subsequently, the resulting solution was constantly stirred for 5 h at 80 °C until it formed a reddish-brown gel. Then, the as-synthesized precursor was dried in oven at 100 °C for 12 h, and was thoroughly milled into fine powder with agate mortar. Finally, the LaFeO_3 catalyst was successfully synthesized by annealing in a muffle furnace at 350 °C for 2 h and then at 700 °C for 2 h at a rate of 2 °C·min⁻¹.

Pure SnS_2 plates were prepared with a simple hydrothermal method.² Firstly, $\text{SnCl}_4 \cdot 5\text{H}_2\text{O}$ (1.7530 g, 5 mmol) and thiourea (2.2836 g, 30 mmol) were completely dissolved in 70 mL of deionized water to obtain a colorless homogeneous solution. Then, the solution was transferred into a 100 mL of Teflon-lined autoclave and heated at 180 °C for 12 h. After cooling to room temperature, the as-obtained yellow resultant was collected, and then washed several times with deionized water and ethanol, finally dried in oven at 80 °C for 12 h.

Characterization

X-ray Powder Diffractometer (Ultima IV, Japan) with a $\text{Cu K}\alpha$ radiation source ($\lambda = 1.5406 \text{ \AA}$) was used to obtain the XRD patterns of the synthesized photocatalysts. All samples were continuously examined with the scanning range of $2\theta = 10^\circ \sim 80^\circ$ at the scanning speed of 15 °·min⁻¹. The FT-IR spectra with the range of 4000 ~ 400 cm⁻¹ were acquired to analyze chemical bonding information of samples by the Fourier Transform Infrared Spectrometer (Nicolet 5700, USA) using the KBr pellets method. The surface morphologies and elemental compositions of the as-synthesized materials were investigated by the Scanning Electron Microscopy (SEM) (FEI Inspect F50, China), High Resolution Transmission Electron Microscopy (HRTEM) and Energy Disperse Spectroscopy (EDS). The N_2 adsorption-desorption test was conducted on the automatic specific surface and porosity analyzer (Autosorb-iQ3, USA) to acquire the specific surface area and pore diameter distribution of the as-obtained samples. The X-ray photoelectron spectroscopy (XPS) test was performed on the X-ray photoelectron

spectrometer (Thermo Scientific K-Alpha, USA) with an Al K α excitation source (1486.6 eV). The binding energy of each element was corrected using adventitious contamination C 1s (284.8 eV) as the standard. The UV-vis diffuse reflectance spectra were recorded by UV-vis spectrophotometer (UV-2600, Japan) equipped with the BaSO₄-coated diffuse emission integrating sphere in the wavelength range of 200 ~ 800 nm.

Photoelectrochemical Experiments (PEC)

The transient photocurrent responses (I-t), electrochemical impedance spectroscopies (EIS) and the Mott-Schottky (MS) measurements were conducted using the electrochemical workstation (CHI660E, China) with the three-electrode system. In the test, the Pt was selected as the counter electrode, Ag/AgCl as the reference electrode, and the sample deposited on ITO as the working electrode. Sodium sulfate aqueous solution (0.50 M) was used as the electrolyte of I-t or MS tests, and the mixed solution of K₃[Fe (CN)₆] (5 mM) and KCl (1 M) was utilized as the electrolyte of EIS tests. And the needed irradiation light source was provided by the 300 W Xe lamp with a 420 nm cutoff filter. The transient photocurrent responses (I-t) were tested with an on-off light interval of 20 seconds for 4 cycles. The electrochemical impedance spectroscopies (EIS) were performed with the given AC amplitude of 5 mV at the frequency range from 100 kHz to 1.0 Hz. The Mott-Schottky (MS) plots were recorded with the potential range of -1.0 ~ 1.0 V at a fixed frequency of 1000 Hz.

Reference formula

The degradation efficiency (*A* %) of CRS met with the following equation (Eq. S1), where *C*₀ is the initial CRS concentration, and *C* is the final CRS concentration at a given time intervals.

$$A \% = \left(1 - \frac{C}{C_0}\right) \times 100 \quad S1$$

The standard deviations could be calculated by the following formula (Eq. S2), where *y*_{*i*} is the experimental data, \bar{y} is the average of the experimental data, and *N* is

the number of experiments.

$$SD = \sqrt{\frac{1}{N-1} \sum_{i=1}^N (y_i - \bar{y})^2} \quad S2$$

The tauc equation is as follow (Eq. S3), where $h\nu$ is light energy, α is absorption coefficient, A is a proportionality constant, E_g is the band gap energy, and $n = 2$ for direct band gap materials of LFO and SN.

$$(\alpha h\nu)^n = A(h\nu - E_g) \quad S3$$

The conduction band (E_{CB}) and valence band (E_{VB}) of LFO and SN were respectively calculated by the following empirical equations (Eq. S4-S5), where X is the absolute electronegativity of the semiconductor ($X = 5.55$ eV for LFO and $X = 4.66$ eV for SN), E_e is the energy of free electrons on the hydrogen scale (about 4.5 eV), E_{CB} is the CB edge potential and E_{VB} is the VB edge potential (vs NHE), and E_g is the band-gap energy of the semiconductor.³

$$E_{CB} = X - E_e - 0.5E_g \quad S4$$

$$E_{VB} = E_{CB} + E_g \quad S5$$

Figure and Table

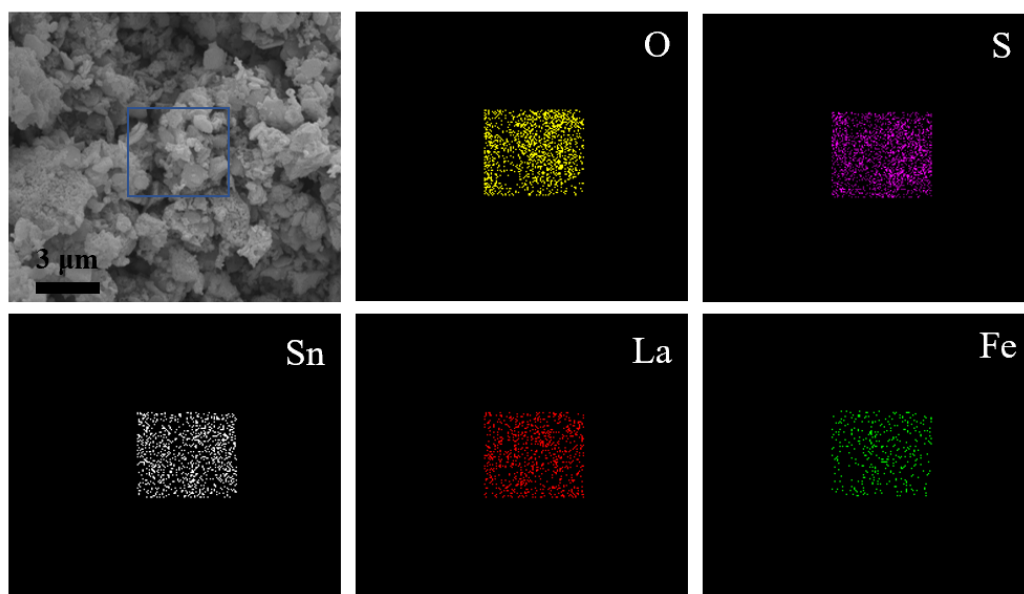


Fig. S1 The elemental mapping images of 20-SN/LFO.

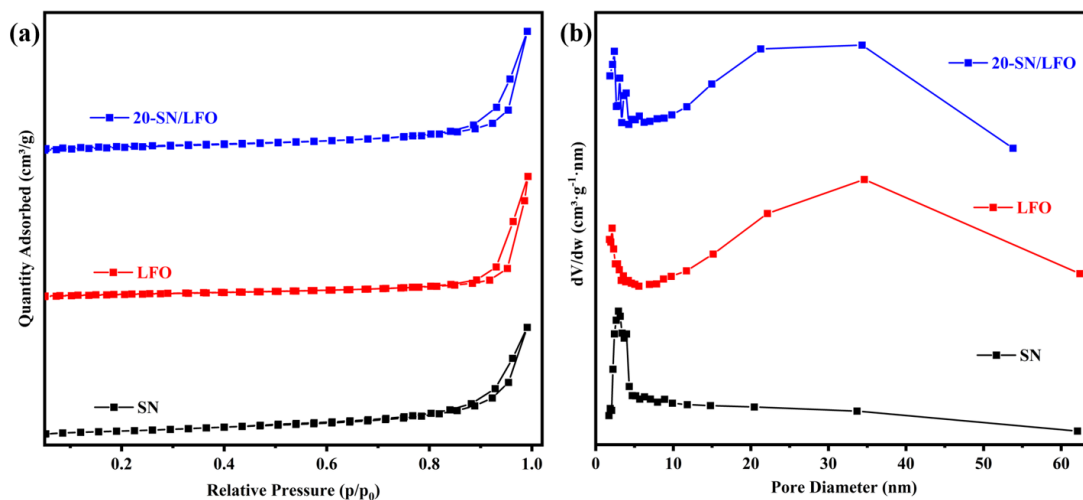


Fig. S2 N₂ adsorption–desorption isotherms (a), BJH desorption pore diameter distribution curves (b) of LFO, SN and 20-SN/LFO.

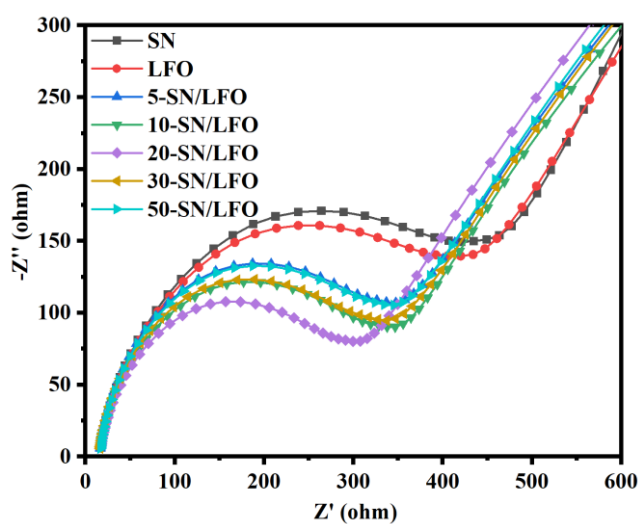


Fig. S3 EIS Nyquist plots of single LaFeO₃, pure SnS₂ and SnS₂/LaFeO₃ composites.

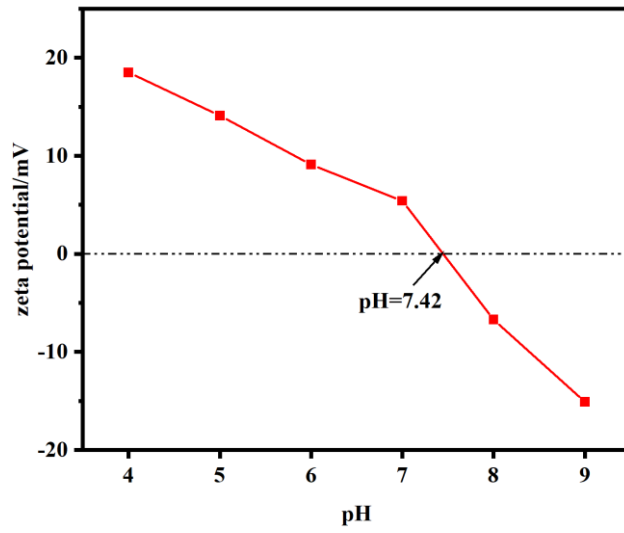


Fig. S4 zeta potentials of 20-SN/LFO sample.

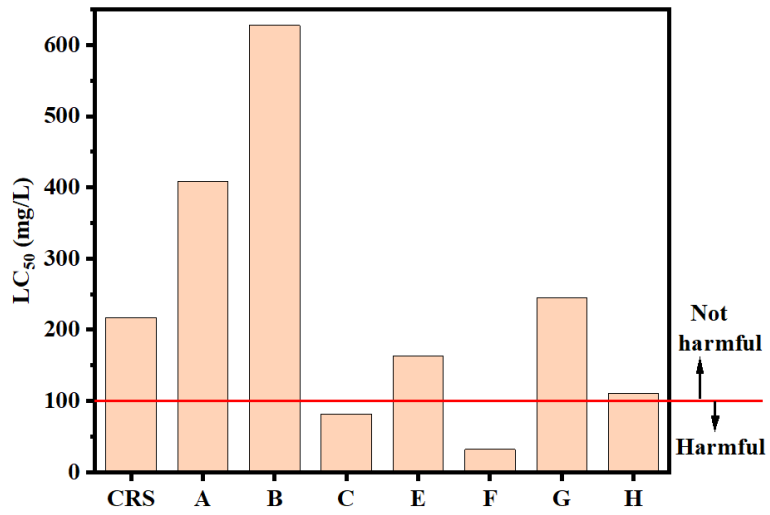


Fig. S5 48-hour LC50 for daphnia magna of CRS and its intermediate products.

Table S1 Chemical structure and relevant information for ceftriaxone sodium.

Name	Ceftriaxone sodium
Formula	$C_{18}H_{16}N_8Na_2O_7S_3$
Structure	
Molecular mass (g mol ⁻¹)	598.54
λ_{max}	240.50 nm

Table S2 Possible intermediate pathway for the photo-Fenton degradation of ceftriaxone sodium.

No.	m/z	Possible degradation pathway	Predicted structure
A	419.41	C-S bond rupture	
B	415.35	C-N bond rupture	
C	282.31	The fracture of β -lactam and loss of carbonyl group	
D	242.25	The fracture of β -lactam	

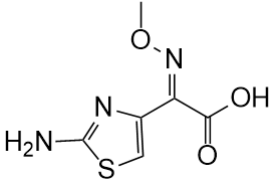
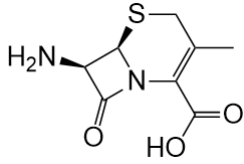
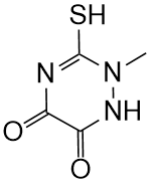
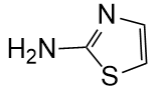
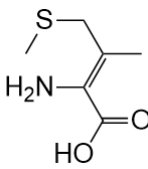
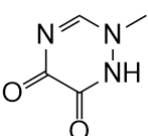
E	210.20	C-N bond rupture	
F	214.24	C-N、C-S bond rupture	
G	159.16	C-S bond rupture	
H	100.14	C-C bond rupture	
I	161.22	The fracture of β -lactam and C-S bond rupture	
J	127.10	C-S bond rupture	

Table S3 The acute toxic criterion (unit: mg L⁻¹).

Acute toxicity ^a	Toxicity grade
LC ₅₀ >100 or EC ₅₀ >100	Not harmful
10< LC ₅₀ <100 or 10< EC ₅₀ <100	harmful
1< LC ₅₀ <10 or 1< EC ₅₀ <10	Toxic
LC ₅₀ <1 or EC ₅₀ <1	Very toxic

^a Criteria set by the Chinese hazard evaluation guidelines for new chemical substances (HJ/T 154–2004)

References

1. Y. Hsu, S. Chang, W. Chung and M. Chang, *Environmental Science and Pollution Research*, 2019, **26**, 26276-26285.
2. J. Luo, X. Zhou, L. Ma, X. Xu, J. Wu and H. Liang, *Materials Research Bulletin*, 2016, **77**, 291-299.
3. A. Kolivand and S. Sharifnia, *International Journal of Energy Research*, 2021, **45**, 2739-2752.